



## 14-3-3 Gene expression in regenerating rat liver after 2/3 partial hepatectomy

D.M. Xue<sup>1,2</sup>, X.Q. Guo<sup>1,2</sup>, R. Chen<sup>1,2</sup>, Z.P. Niu<sup>1,2</sup> and C.S. Xu<sup>1,2</sup>

<sup>1</sup>College of Life Science, Henan Normal University, Xinxiang, Henan, China

<sup>2</sup>Key Laboratory for Cell Differentiation Regulation, Xinxiang, Henan, China

Corresponding author: C.S. Xu

E-mail: cellkeylab@126.com

Genet. Mol. Res. 14 (1): 2023-2030 (2015)

Received February 11, 2014

Accepted August 4, 2014

Published March 20, 2015

DOI <http://dx.doi.org/10.4238/2015.March.20.12>

**ABSTRACT.** 14-3-3 Proteins are a ubiquitous family of molecules that participate in protein kinase signaling pathways in all eukaryotic cells. Functioning as phosphoserine/phosphothreonine-binding modules, 14-3-3 proteins participate in the phosphorylation-dependent protein-protein interactions that control progression through the cell cycle, initiation and maintenance of DNA damage checkpoints, activation of MAP kinases, prevention of apoptosis, and coordination of integrin signaling and cytoskeletal dynamics. During liver regeneration after partial hepatectomy, normally quiescent hepatocytes undergo hypertrophy and proliferation to restore the liver mass. In this study, we investigated the expression patterns of 14-3-3 mRNAs in regenerating rat liver after 2/3 partial hepatectomy using real-time quantitative reverse transcription-polymerase chain reaction. All mRNAs of the 14-3-3 7 isotypes were expressed at 10 time points. Upregulation of 14-3-3 $\xi$  mRNA expression and downregulation of 14-3-3 $\sigma$  mRNA expression from 0 to 6 h may play important roles in the entry into S-phase. Downregulation of 14-3-3 $\beta$ ,  $\gamma$ ,  $\sigma$ ,  $\eta$ , and  $\tau$  mRNA expression from 24 to 30 h, when compared to 0 h, was closely related to entry into mitosis.

**Key words:** 14-3-3 mRNA; Liver regeneration; Reverse transcription-polymerase chain reaction

## INTRODUCTION

The liver has a remarkable capacity to regenerate after various types of injuries. The liver consists of numerous cell types, including hepatocytes, Kupffer cells, stellate cells, sinusoidal endothelial cells, and biliary epithelial cells (Kang et al., 2012). However, hepatocytes, which carry out most of the metabolic and synthetic functions in the liver, account for approximately 80% of the liver weight and around 70% of all liver cells (Si-Tayeb et al., 2010). In severely damaged liver with impaired hepatocyte proliferation, liver stem/progenitor cells, which have the potential to differentiate into both hepatocytes and biliary epithelial cells, proliferate and are thought to contribute to regeneration (Alison et al., 2009). In contrast, regeneration after partial hepatectomy (PH) does not require such stem/progenitor cells. The remnant tissue undergoes compensatory hyperplasia to recover the original liver mass within approximately 1 week in rodents (Michalopoulos, 2007). The multi-lobular structure of the rodent liver allows the surgical resection of a lobe of choice to acquire different degrees of liver mass loss. Upon 30% PH, the liver recovers its original mass by increasing the size of hepatocytes, but neither the cell number nor the nuclear number of hepatocytes changes. In contrast, when 70% of the liver is removed, hypertrophy of hepatocytes occurs in a few hours after PH, followed by cellular proliferation. A combination of increased cellular size and hepatocyte number allows for the recovery of liver mass after 70% PH. Because resection of lobes does not induce damage to the remnant liver tissue, PH is considered to be an excellent experimental model for regeneration (Miyaoaka and Miyajima, 2013).

Members of the 14-3-3 protein family form a group of highly conserved 30-kDa acidic proteins expressed in a wide range of organisms and tissues. This family consists of 7 isoforms in human and rodent tissues ( $\beta/\alpha$ ,  $\gamma$ ,  $\xi/\delta$ ,  $\sigma$ ,  $\epsilon$ ,  $\eta$ ,  $\tau/\theta$ ) and plays crucial roles in regulating multiple cellular processes, including the maintenance of cell cycle checkpoints and DNA repair, prevention of apoptosis, onset of cell differentiation and senescence, and coordination of cell adhesion and motility. Functioning as phosphoserine/phosphothreonine-binding modules, 14-3-3 proteins participate in phosphorylation-dependent protein-protein interactions (Wilker and Yaffe, 2004). Their expression is tissue-specific.

Cell division and apoptosis occur during liver regeneration after 2/3 PH (Sakamoto et al., 1999); thus, the 14-3-3 protein family may be closely related to liver regeneration. In this study, we investigated the pattern of 14-3-3 mRNA expression during liver regeneration after 2/3 PH using real-time quantitative reverse transcription (qRT)-polymerase chain reaction (PCR).

## MATERIAL AND METHODS

### Animals and PH model

Sprague-Dawley male rats ( $200 \pm 10$  g) were obtained from the Animal Center of Henan Normal University, China. Animals were allowed access to food and water *ad libitum*. Ether inhalation was used to anesthetize animals. In the PH model, the median and left lateral lobes (accounting for 2/3 of the total liver mass) were resected (Stolz et al., 1999). The remaining liver lobes were obtained at 0, 2, 6, 12, 24, 30, 36, 72, 120, and 168 h after PH. All liver samples were promptly frozen in liquid nitrogen and stored at  $-80^{\circ}\text{C}$ . All animals were housed in the animal facility of Animal Center of Henan Normal University, and all procedures performed were conducted according to the Animal Protection Law of China.

## Real-time qRT-PCR analysis

Total RNA from frozen liver samples were extracted according to TaKaRa RNAiso™ Plus specifications (Shiga, Japan). Real-time qRT-PCR was conducted using the CFX96™ Real-Time System (Bio-Rad, Hercules, CA, USA). Gene-specific primers were designed based upon the sequences in GenBank. Sequences and expected PCR product lengths are shown in Table 1. The specificity of the amplified products was evaluated by analyzing the dissociation curves. As a control with the time point of 0 h and the endogenous control *Actb* gene, relative expression levels of the genes were calculated using the formula  $Ratio_{(test/calibrator)} = E^{\Delta C_T(calibrator) - \Delta C_T(test)}$ . Real-time qPCR amplifications were carried out in a final volume of 25  $\mu$ L, which contained 12.5  $\mu$ L 2X SYBR Premix Ex Taq™ (TaKaRa), 1  $\mu$ L diluted template including 200 ng cDNA, 11.0  $\mu$ L PCR-grade water, and 0.25  $\mu$ L of each primer. PCR conditions were as follows: predenaturation at 95°C for 30 s, 39 cycles of denaturation at 94°C for 15 s, annealing at 56°C for 20 s, and elongation at 72°C for 20 s.

**Table 1.** Forward (F) and reverse (R) primer sequences, size of cDNA, and GenBank accession number of the factors investigated.

Gene symbol	Product	Primer sequence (5'-3')	Length (bp)	GenBank
<i>Actb</i> *	$\beta$ -actin	F: ACATCCGTAAGACCTCTATGCCAACA R: GTGCTAGGAGCCAGGGCAGTAATCT	125	V01217.1
<i>Ywhab</i>	14-3-3 $\beta/\alpha$	F: AGCCATTGCTGAGTTGGACA R: TGACGTCCACAGGGTGAGAT	195	NM_019377.1
<i>Ywhag</i>	14-3-3 $\gamma$	F: AAGGCAGTCTTCGGTTTCCT R: CTGTCACGTTCTTCATGGCCG	232	NM_019376.2
<i>Ywhaz</i>	14-3-3 $\xi/\delta$	F: CCCACTCCGGACACAGAATA R: TGTCATCGTATCGCTCTGCC	236	NM_013011.3
<i>LOC298795</i>	14-3-3 $\sigma$	F: CTGAGAGACAACCTGACGCT R: TGAGATTCAATTTCCAGCCCT	215	NM_001013941.1
<i>Ywhae</i>	14-3-3 $\epsilon$	F: CCGAGCGATACGACGAAATG R: TCAACTGTCAGCTCCACGTC	158	NM_031603.1
<i>Ywhah</i>	14-3-3 $\eta$	F: CATGAAGCCGGTGACAGAGC R: CCATCTGCCATGGTTTCTGC	189	NM_013052.1
<i>Ywhaq</i>	14-3-3 $\tau/\theta$	F: GCTAAAACGGCTTTTGATGAAGC R: ATGCCTTATGTTCTCAGCCCC	154	NM_013053.1

\*Endogenous control gene.

## Statistical analysis

Statistical analyses were carried out using SPSS 16.0 (SPSS, Inc., Chicago, IL, USA). All data are reported as means  $\pm$  standard deviation (N = 3). The *t*-test was used for analysis of variance. A P value less than 0.05 was considered to be statistically significant.

## RESULTS

The entire process of rat liver regeneration following PH is typically complete within 5-7 days. Here, we investigated 14-3-3 mRNA levels during this process. The expression of 14-3-3  $\beta/\alpha$  mRNA showed a variable pattern during the regeneration process after PH. At 0 h after PH, the mRNA level was the highest. At 24 h, the lowest value was observed. At 168 h (7 days), the level was the nearest to that at 0 h, and showed no significant difference when compared to that at 0 h (Figure 1).

Expression of 14-3-3 $\gamma$  mRNA showed a wavy pattern during the regenerative process after PH. At 0 h after PH, the mRNA level was the highest. At 120 h, the mRNA level reached the lowest value observed (Figure 2).

Expression of 14-3-3 $\xi/\delta$  mRNA increased rapidly from 0 h after PH and peaked at 6 h, then decreased until 72 h. From 72 to 120 h, the mRNA level rapidly increased again. From 120 to 168 h, the increase slowed. At 6 h after PH, the mRNA level was the highest. At 72 h, the level reached the lowest value. At 168 h, the mRNA level was the closest to that at 0 h (Figure 3).

Expression of 14-3-3 $\sigma$  mRNA decreased dramatically from 0 to 2 h after PH and then showed wavy oscillations. At 0 h after PH, the mRNA level was the highest. At 6 h, the mRNA level reached the lowest value. At 168 h, the level was much lower than that at 0 h (Figure 4).

Expression of 14-3-3 $\epsilon$  mRNA increased from 0 h after PH with a peak at 24 h, and then decreased until 72 h. From 72 to 120 h, the mRNA level increased. After this point, expression reached a plateau. At 168 h, the mRNA level was the closest to that at 0 h (Figure 5).

Expression of 14-3-3 $\eta$  mRNA decreased rapidly from 0 to 2 h after PH and then showed small amplitude oscillations (Figure 6).

Expression of 14-3-3 $\tau/\theta$  mRNA decreased sharply to nearly 0 from 0 to 2 h after PH, and then maintained a constant level (Figure 7).

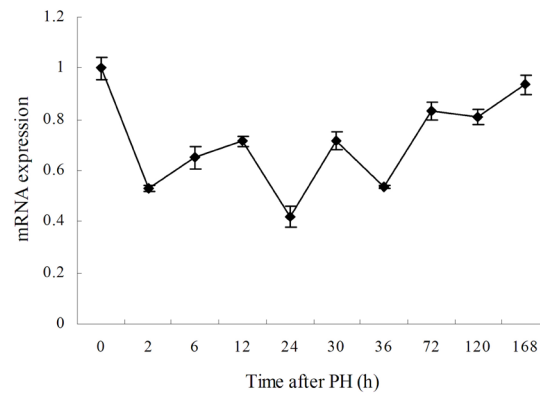


**Figure 1.** mRNA expression of *Ywhab* (14-3-3 $\beta/\alpha$ ) at various time points after partial hepatectomy (PH).

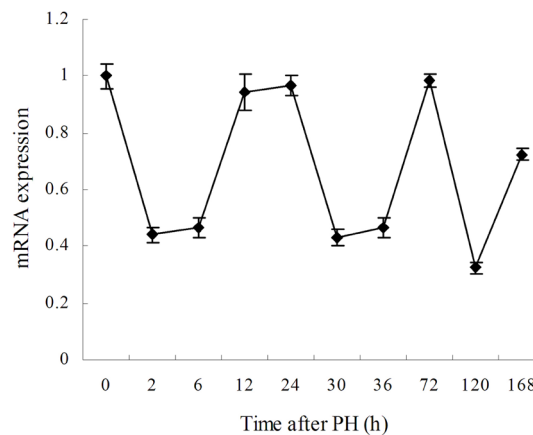


**Figure 2.** mRNA expression of *Ywhag* (14-3-3 $\gamma$ ) at various time points after partial hepatectomy (PH).

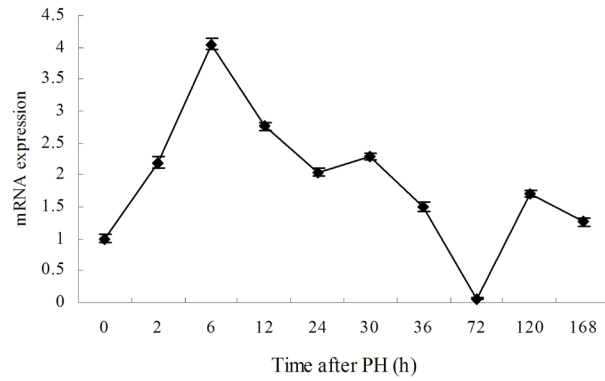


**Figure 3.** mRNA expression of *Ywhaz* (14-3-3 $\xi/\delta$ ) at various time points after partial hepatectomy (PH).

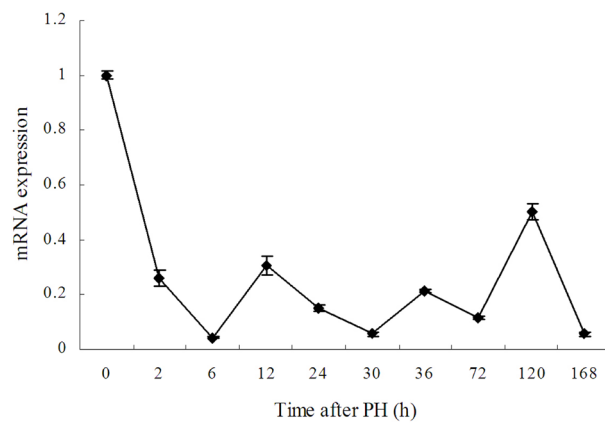


**Figure 4.** mRNA expression of *LOC298795* (14-3-3 $\sigma$ ) at various time points after partial hepatectomy (PH).

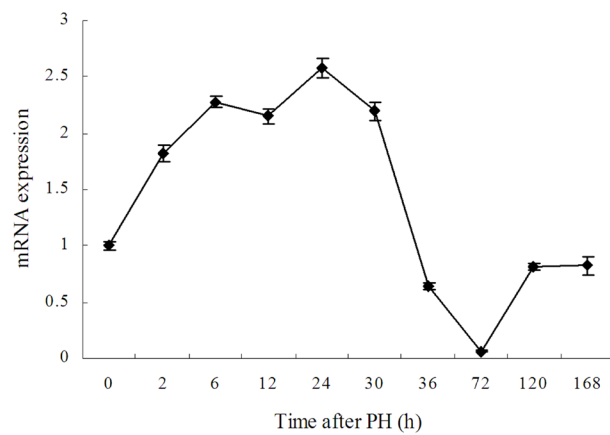


**Figure 5.** mRNA expression of *Ywhae* (14-3-3 $\epsilon$ ) at various time points after partial hepatectomy (PH).

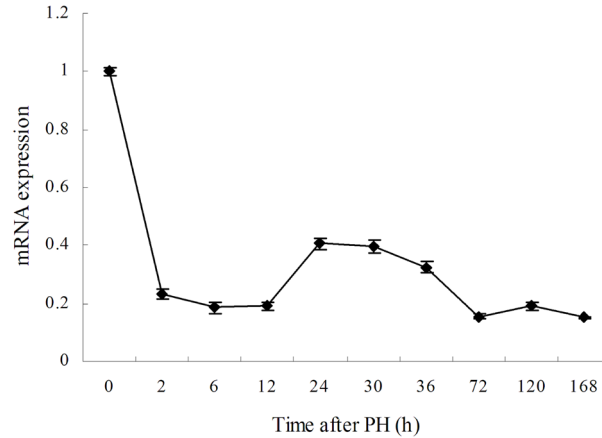


**Figure 6.** mRNA expression of *Ywhah* (14-3-3 $\eta$ ) at various time points after partial hepatectomy (PH).

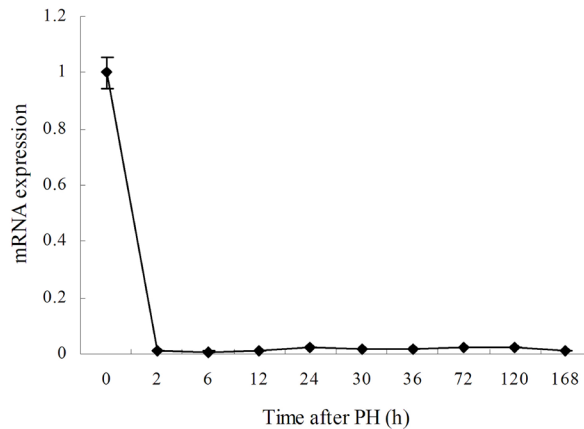


**Figure 7.** mRNA expression of *Ywhaq* (14-3-3 $\tau/\theta$ ) at various time points after partial hepatectomy (PH).

## DISCUSSION

Liver regeneration has been studied extensively, but many important fundamental mechanisms remain undefined, such as the mechanisms of cellular hypertrophy, cell division, nuclear division, ploidy changes, and organ size control (Miyaoka and Miyajima, 2013). It is thought that during liver regeneration after PH, normally quiescent hepatocytes undergo 1-2 rounds of replication to restore the liver mass by a process of compensatory hyperplasia (Duncan et al., 2009). Recent studies have reported that during liver regeneration after 2/3 PH, although nearly all hepatocytes enter into S-phase, not all hepatocytes divide. Upon 2/3 PH, the liver recovers its original mass through a combination of increased cell size and hepatocyte number (Miyaoka and Miyajima, 2013).

14-3-3 Proteins are involved in regulating the G<sub>1</sub>/S-phase transition through several mechanisms. Cell division cycle 25A is a central regulator of S-phase entry, which dephos-

phosphorylates cyclin-dependent kinase 2 (CDK2) on its inhibitory phosphates Thr-14 and Tyr-15 and is inactivated by cytoplasmic sequestration by 14-3-3 $\epsilon$  (Chen et al., 2003). Furthermore, a direct association between 14-3-3 $\sigma$  and CDK2 and CDK4 negatively regulates S-phase entry (Laronga et al., 2000). 14-3-3 $\beta$ ,  $\gamma$ ,  $\xi$ ,  $\epsilon$ ,  $\eta$ , and  $\tau$  may bind to p27<sup>KIP1</sup>, which mediates G<sub>1</sub>-arrest by inhibiting cyclin E-CDK2 complexes. Through this association, 14-3-3 proteins may promote CDK activation and cell cycle progression (Sekimoto et al., 2004). The upregulation of 14-3-3 $\xi$  mRNA expression and downregulation of 14-3-3 $\sigma$  mRNA expression from 0 to 6 h may play important roles in S-phase entry.

14-3-3 Proteins are also involved in the regulation of the G<sub>2</sub>/M-phase transition by several mechanisms. In mammalian cells, an obligate step for entry into mitosis is the activation of CDC2 kinase. During S-phase, the activity of CDC2 is suppressed through phosphorylation by the WEE1 and MYT1/MIK1 kinases on the residues Thr-14 and Thr-15. The phosphatase CDC25C dephosphorylates these residues, resulting in CDC2 activation and initiating the entry into mitosis (Gautier et al., 1991). CDC25C activity is repressed by phosphorylation by checkpoint kinase 1 through subsequent binding to 14-3-3 proteins and cytoplasmic sequestration. This leads to increased CDC2 phosphorylation and lower activity of CDC2 and inhibition of mitotic entry (Sanchez et al., 1997). Not all 14-3-3 family members can bind and regulate CDC25C. Dalal et al. (2004) tested 7 different 14-3-3 protein isoforms and found that only 14-3-3 $\epsilon$  and  $\gamma$  specifically form a complex with CDC25C in U2OS cells to inhibit CDC25C from inducing premature chromatin condensation. Qi and Martinez (2003) found that CDC25C interacts with 14-3-3 $\xi$  and  $\tau$  in lung adenocarcinoma A549 cells. In contrast, 14-3-3 $\sigma$  does not bind to CDC25C, but nonetheless blocks premature chromatin condensation. Presumably, 14-3-3 $\sigma$  induces G<sub>2</sub>-arrest by sequestering CDC2-cyclin B complexes in the cytoplasm, thereby separating them from nuclear substrates (Chan et al., 1999). CDC25B is also regulated through its association with 14-3-3 proteins, as phosphorylation of Ser-323 and subsequent 14-3-3 binding inhibits CDC25B activity. CDC25B is bound by different members of the 14-3-3 family; it interacts with 14-3-3 $\beta$ ,  $\xi$ , and  $\eta$  in a yeast 2-hybrid assay and with 14-3-3 $\xi$ ,  $\eta$ , and  $\sigma$  *in vivo* (Mils et al., 2000). A central regulator of CDC2 activity, WEE1 kinase, is also regulated by 14-3-3 proteins. WEE1 inactivates the CDC2-cyclin B complex during interphase by phosphorylating CDC2 on Tyr-15. Co-expression of WEE1 and 14-3-3 $\beta$  increases the kinase activity of WEE1, resulting in G<sub>2</sub>/M arrest (Wang et al., 2000).

The complex regenerating process can be divided into 3 distinct phases: initiation, proliferation, and termination. In rats, within less than 15 min after PH, hepatocytes exit quiescence and enter the G<sub>1</sub>-phase. The first wave of hepatocyte proliferation following PH is synchronous. The peak of DNA synthesis is observed at 22-24 h, followed by a peak in mitosis at 28-30 h (Corlu and Loyer, 2012). In conclusion, downregulation of 14-3-3 $\beta$ ,  $\gamma$ ,  $\sigma$ ,  $\eta$ , and  $\tau$  mRNA expression from 24 to 30 h, when compared to 0 h, is closely related to entry into mitosis.

Because of the multilobe structure of the rodent liver, the median and left lateral lobes (representing 2/3 of the liver mass) can be removed using an easy surgical procedure without causing tissue damage to the residual 2 lobes. The latter grows in size to restore an aggregate equivalent to the mass of the original 5 lobes. The process is complete within 5-7 days after surgery (Michalopoulos, 2007). At 168 h (7 days), the expression level of 14-3-3 $\beta$ ,  $\gamma$ ,  $\xi$ , and  $\epsilon$  was close to the value at 0 h; however, the level of 14-3-3 $\sigma$ ,  $\eta$ , and  $\tau$  was much lower than the value at 0 h. Thus, 14-3-3 proteins may be functionally redundant and compensate for each other.

## ACKNOWLEDGMENTS

Research supported by the Base and Frontier Technology Research Project of Henan Province (#132300410135), the Foundation for Doctor of Henan Normal University (#qd13031), the National Basic Research “973” Pre-Research Program of China (#2012CB722304), and the Biological Key Discipline of Henan Province.

## REFERENCES

- Alison MR, Islam S and Lim S (2009). Stem cells in liver regeneration, fibrosis and cancer: the good, the bad and the ugly. *J. Pathol.* 217: 282-298.
- Chan TA, Hermeking H, Lengauer C, Kinzler KW, et al. (1999). 14-3-3Sigma is required to prevent mitotic catastrophe after DNA damage. *Nature* 401: 616-620.
- Chen MS, Ryan CE and Piwnicka-Worms H (2003). Chk1 kinase negatively regulates mitotic function of Cdc25A phosphatase through 14-3-3 binding. *Mol. Cell. Biol.* 23: 7488-7497.
- Corlu A and Loyer P (2012). Regulation of the G<sub>1</sub>/S transition in hepatocytes: involvement of the cyclin-dependent kinase Cdk1 in the DNA replication. *Int. J. Hepatol.* 2012: 689324.
- Dalal SN, Yaffe MB and DeCaprio JA (2004). 14-3-3 family members act coordinately to regulate mitotic progression. *Cell Cycle* 3: 672-677.
- Duncan AW, Dorrell C and Grompe M (2009). Stem cells and liver regeneration. *Gastroenterology* 137: 466-481.
- Gautier J, Solomon MJ, Booher RN, Bazan JF, et al. (1991). cdc25 is a specific tyrosine phosphatase that directly activates p34cdc2. *Cell* 67: 197-211.
- Kang LI, Mars WM and Michalopoulos GK (2012). Signals and cells involved in regulating liver regeneration. *Cells* 1: 1261-1292.
- Laronga C, Yang HY, Neal C and Lee MH (2000). Association of the cyclin-dependent kinases and 14-3-3sigma negatively regulates cell cycle progression. *J. Biol. Chem.* 275: 23106-23112.
- Michalopoulos GK (2007). Liver regeneration. *J. Cell. Physiol.* 213: 286-300.
- Mils V, Baldin V, Goubin F, Pinta I, et al. (2000). Specific interaction between 14-3-3 isoforms and the human CDC25B phosphatase. *Oncogene* 19: 1257-1265.
- Miyaoka Y and Miyajima A (2013). To divide or not to divide: revisiting liver regeneration. *Cell Div.* 8: 8.
- Qi W and Martinez JD (2003). Reduction of 14-3-3 proteins correlates with increased sensitivity to killing of human lung cancer cells by ionizing radiation. *Radiat. Res.* 160: 217-223.
- Sakamoto T, Liu Z, Murase N, Ezure T, et al. (1999). Mitosis and apoptosis in the liver of interleukin-6-deficient mice after partial hepatectomy. *Hepatology* 29: 403-411.
- Sanchez Y, Wong C, Thoma RS, Richman R, et al. (1997). Conservation of the Chk1 checkpoint pathway in mammals: linkage of DNA damage to Cdk regulation through Cdc25. *Science* 277: 1497-1501.
- Sekimoto T, Fukumoto M and Yoneda Y (2004). 14-3-3 suppresses the nuclear localization of threonine 157-phosphorylated p27(Kip1). *EMBO J.* 23: 1934-1942.
- Si-Tayeb K, Lemaigre FP and Duncan SA (2010). Organogenesis and development of the liver. *Dev. Cell* 18: 175-189.
- Stolz DB, Mars WM, Petersen BE, Kim TH, et al. (1999). Growth factor signal transduction immediately after two-thirds partial hepatectomy in the rat. *Cancer Res.* 59: 3954-3960.
- Wang Y, Jacobs C, Hook KE, Duan H, et al. (2000). Binding of 14-3-3beta to the carboxyl terminus of Wee1 increases Wee1 stability, kinase activity, and G<sub>2</sub>-M cell population. *Cell Growth Differ.* 11: 211-219.
- Wilker E and Yaffe MB (2004). 14-3-3 Proteins - a focus on cancer and human disease. *J. Mol. Cell. Cardiol.* 37: 633-642.